Supplementary Material 1 - Mapping Hand Muscle Myoelectric Activity into Finger and Wrist Kinematics During Natural Dynamic Movements with Deep Learning Prediction Models

Marcus Panchal, Simone Tanzarella, Moon Ki Jung and Dario Farina

November 2022

A Motion Tasks Performed

Table 1 describes the motion tasks recorded within our custom collected dataset. Each One and Two DoF motion is performed for each digit individually as described in the table. Figure 1 illustrates how the motions were performed for a single repetition during each motion task recording, depending on if the recording was for 30 seconds or longer. For recordings lasting 30 seconds, each repetition consisted of moving from neutral hand position to the desired extreme of the motion by 2.5 seconds, holding the extreme for 1 second, and then returning to neutral position by 6 seconds. Recordings lasting longer than 30 seconds were similar, however each repetition is double the length and involves both the positive and negative extremes of the joint (e.g full flexion and full extension of the MCP Joint).

Table 1: Motion Tasks Recorded

Task Name	Digits Involved in Motion	Recording Time	Subjects	Motion Group
PIP Flexion	Index, Middle, Little, Thumb	30 Seconds	1, 4	One DoF
MCP Flexion-Extension	Index, Middle, Ring, Little, Thumb	1 Minute	1, 2, 3, 4, 5	One DoF
MCP Abduction-Adduction	Thumb	1 Minute	1, 2, 3, 4, 5	One DoF
Opposition	Thumb	30 Seconds	1, 2, 3, 4, 5	One DoF
Wrist Flexion-Extension	Wrist	1 Minute	1, 2, 3, 4, 5	One DoF
MCP Flexion-Extension + Wrist Flexion	Index, Middle, Ring, Little, Thumb	1 Minute	1, 2, 3, 4, 5	Two DoF
MCP Flexion-Extension + Wrist Extension	Index, Middle, Ring, Little, Thumb	1 Minute	1, 2, 3, 4, 5	Two DoF
Hand Grasp	All Digits	30 Seconds	1, 2, 3, 4, 5	Natural Motions
Three Finger Pinch	Index, Middle, Thumb	30 Seconds	1, 2, 3, 4, 5	Natural Motions
Two Finger Pinch	Index, Thumb	30 Seconds	1, 2, 3, 4, 5	Natural Motions
Sign Language Letters	All Digits	4 Minutes	1, 2, 3, 4, 5	Sign Language

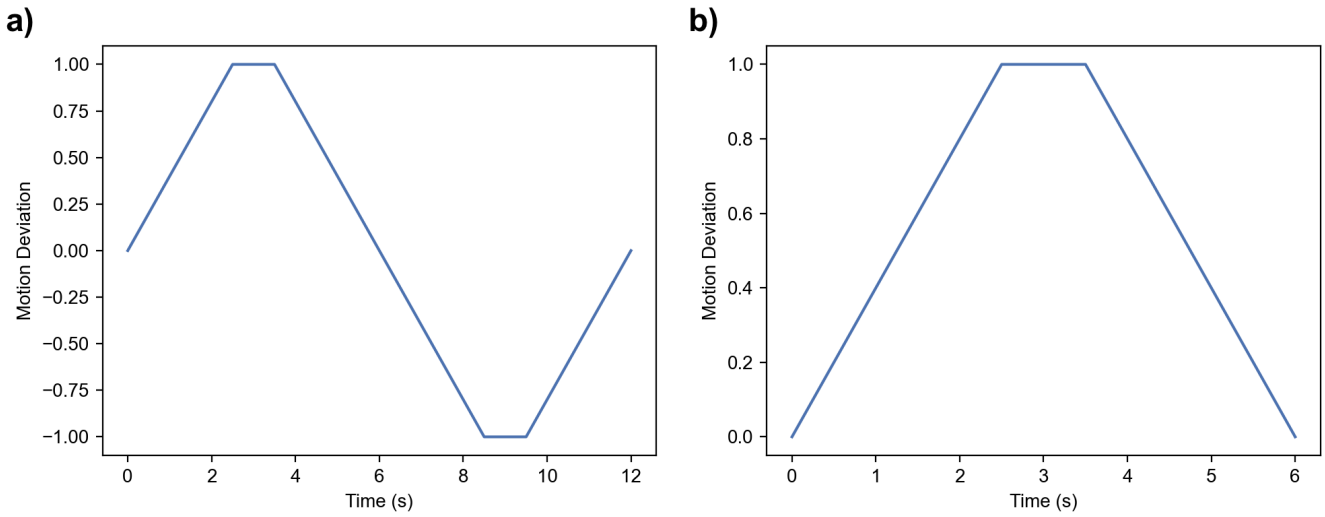


Figure 1: Intended Motion Deviation during Motion Task Recordings for tasks that were recorded for longer than 30 seconds **a)** and for tasks that were recorded for 30 second exactly **b)**. Each recording consisted of 5 repetitions of the motion task. Motion Deviation is 0 at the neutral position of the hand and 1 or -1 at the extremes of the motion.

B Post Processing of Motion Capture Data

During marker labelling it was noted that some markers did not appear in certain recordings, possibly due to limitations in the motion capture system used. In order to compensate for the gap in information due to the missing markers, we used the recordings where these markers were present to estimate their position. For each marker, we calculate a mean positional vector relative to a nearby anatomically connected marker that was present for all the files (i.e if the DIP joint marker was missing the mean positional vector would have been calculated relative to the nearby PIP joint marker). This allowed us to calculate where the missing markers would have been in the recordings based on the position of the other markers. Our correction technique was performed per subject to account for inter-subject anatomical variability, increasing the accuracy.

To further remove noise from each coordinate of the marker tracks, a 3rd order interpolating spline was fitted to each dimension of the kinematic tracks. Regions of the spline that displayed a derivative above an empirically chosen threshold (Threshold = 0.3) were removed, as these were deemed noisy regions (i.e movements of the marker in an axis not deemed accurate or probable). This resulted in the removal of further noisy kinematic segments, however it did leave small kinematic segments of noise that had a derivative of 0. In order to remove these, an empirical threshold length of 6 samples was used to distinguish these segments from short segments of actual kinematic data (which were more likely to be longer in length).

The resulting kinematic data from the above stages now contained various gaps within each track where there was no positional data. Three gap filling techniques [1] were applied to the channels in order to accurately fill these empty regions to provide continuous kinematic data for all markers:

- **Rigid Body Filling** - (treating a group of markers as a rigid body, the missing kinematic data can be determined from the trajectories of the other markers that are part of the same rigid body, assuming that they are intact)
- **Kinematic Filling** - (treating a group of markers as a segment, the missing kinematic data can be determined from the rotation and orientation of the segment/other markers from before and after the missing time steps)
- **Interpolated Spline Filling** - (mathematically fitting a 3rd order spline to all the available kinematic data points and then adding data points that lie on the spline at the missing time steps)

Each kinematic marker track was then passed through a second order Butterworth low pass filter (cutoff frequency of 6Hz), in order to smooth and further remove any noise. The Motion capture data was then up-sampled to 2048 Hz by fitting an interpolated spline. This allowed for synchronisation with the sEMG data, with the kinematics cropped to the same length and alignment as mentioned previously.

After calculation of the joint angle time series from the marker kinematics, there remained some areas of inaccuracy and noise. We therefore performed all of the above processing steps again on this newly calculated angle data. This included an additional step: removing and interpolating over any data points that were outside the range $\mu_{angle} \pm 3 * \sigma_{angle}$ for each angle series.

C Joint Angle Calculation

For the estimation of wrist flexion-extension angle, both the hand and the forearm coordinate systems need to be defined.

The following are the basis vectors for the hand coordinate system:

$$\begin{aligned}
\overrightarrow{O_{hand}} &= \overrightarrow{M3} \\
\overrightarrow{MID_{wrist}} &= \frac{\overrightarrow{Rad} + \overrightarrow{Uln}}{2} \\
\overrightarrow{LAT_{hand}} &= \overrightarrow{I3} - \overrightarrow{O_{hand}} \\
\overrightarrow{Y_{hand}} &= \frac{\overrightarrow{MID_{wrist}} - \overrightarrow{O_{hand}}}{\|\overrightarrow{MID_{wrist}} - \overrightarrow{O_{hand}}\|} \\
\overrightarrow{X_{hand}} &= \frac{\overrightarrow{Y_{hand}} \times \overrightarrow{LAT_{hand}}}{\|\overrightarrow{Y_{hand}} \times \overrightarrow{LAT_{hand}}\|} \\
\overrightarrow{Z_{hand}} &= \frac{\overrightarrow{X_{hand}} \times \overrightarrow{Y_{hand}}}{\|\overrightarrow{X_{hand}} \times \overrightarrow{Y_{hand}}\|}
\end{aligned} \tag{1}$$

The following are the basis vectors for the arm coordinate system:

$$\begin{aligned}
\overrightarrow{O_{arm}} &= \overrightarrow{MID_{wrist}} \\
\overrightarrow{MID_{elbow}} &= \frac{\overrightarrow{EpicM} + \overrightarrow{EpicL}}{2} \\
\overrightarrow{LAT_{arm}} &= \overrightarrow{Rad} - \overrightarrow{O_{arm}} \\
\overrightarrow{Y_{arm}} &= \frac{\overrightarrow{MID_{elbow}} - \overrightarrow{O_{arm}}}{\|\overrightarrow{MID_{elbow}} - \overrightarrow{O_{arm}}\|} \\
\overrightarrow{X_{arm}} &= \frac{\overrightarrow{Y_{arm}} \times \overrightarrow{LAT_{arm}}}{\|\overrightarrow{Y_{arm}} \times \overrightarrow{LAT_{arm}}\|} \\
\overrightarrow{Z_{arm}} &= \frac{\overrightarrow{X_{arm}} \times \overrightarrow{Y_{arm}}}{\|\overrightarrow{X_{arm}} \times \overrightarrow{Y_{arm}}\|}
\end{aligned} \tag{2}$$

Then the coordinate systems of the arm and the hand segments can be defined:

$$\begin{aligned}
R_{hand} &= \begin{bmatrix} | & | & | \\ \overrightarrow{X_{hand}} & \overrightarrow{Y_{hand}} & \overrightarrow{Z_{hand}} \\ | & | & | \end{bmatrix} \\
R_{arm} &= \begin{bmatrix} | & | & | \\ \overrightarrow{X_{arm}} & \overrightarrow{Y_{arm}} & \overrightarrow{Z_{arm}} \\ | & | & | \end{bmatrix}
\end{aligned} \tag{3}$$

The transformation matrix between the arm coordinate system and the hand coordinate system is defined as follows:

$$T_{ah} = R_{arm}^{T} \cdot R_{hand} \tag{4}$$

This transformation matrix can be decomposed into the ZYX sequence Euler angles. Wrist flexion-extension angle is the first Euler angle decomposed with respect to the Z axis.

For the individual finger joint flexion-extension angles, it is possible to use a common function to estimate the values by using 3 adjacent markers:

$$\begin{aligned}
flexion\,(p0, p1, p2) &= cos^{-1}\left(\frac{\overrightarrow{p1 - p0} \cdot \overrightarrow{p2 - p1}}{\|\overrightarrow{p1 - p0}\| \cdot \|\overrightarrow{p2 - p1}\|}\right) \\
MCP1 &= flexion\,(Rad, T3, T2) \\
MCP2 &= flexion\,(Rad, I3, I2) \\
MCP3 &= flexion\,(Rad, M3, M2) \\
MCP4 &= flexion\,(Uln, R3, R2) \\
MCP5 &= flexion\,(Uln, L3, L2) \\
PIP1 &= flexion\,(T3, T2, T1) \\
PIP2 &= flexion\,(I3, I2, I1) \\
PIP3 &= flexion\,(M3, M2, M1) \\
PIP4 &= flexion\,(R3, R2, R1) \\
PIP5 &= flexion\,(L3, L2, L1)
\end{aligned} \tag{5}$$

D Deep Learning Model Architectures

Within our work we devised a number of variants of our base deep learning model architecture. Table 2 outlines a summary of the differences between these variants and their parameters. The symbols $\boldsymbol{\alpha}$, $\boldsymbol{\beta}$ and $\boldsymbol{\gamma}$ refer to the number of inception resnet 3D/2D blocks [2] in the feature extractor architecture, number of LSTM layers and number of dense fully connected layers in the final combinatory model, respectively.

Table 2: Model Architecture Summary.

Model Name	α	β	γ	No. of Grid Inputs	Grid Input Shape	Modifications from Base Model
InceptionConvLSTM	8	2	2	6	13x5x205	-
InceptionIntrinsic	8	2	2	4	13x5x205	Only the Intrinsic HDsEMG Grids are used as Input
InceptionModifiedCombination	8	2	3	6	13x5x205	The LSTM layers ($\boldsymbol{\beta}$) are incorporated into the Feature Extractor Model Feature Extractor Models directly predict only the angles that their input muscles actuate
InceptionExtrinsic	8	2	2	2	13x5x205	Only the Extrinsic HDsEMG Grids are used as Input
InceptionLargerModel	12	2	2	6	13x5x205	The number of Inception Resnet Blocks is increased in the Feature Extractor Model

E Classification Results

Full classification results, including Accuracy and F1 score, for each model variant and digit are found in Table 3. Digits are also further subdivided into Metacarpo-phalgeal (MCP) and Proximal Inter-phalangeal (PIP) joints within the analysis.

Table 3: Model and Joint Classification Accuracy and F1 Scores.

Models		**InceptionConvLSTMHybrid**		**InceptionIntrinsic**		**InceptionModifiedCombination**		**InceptionExtrinsic**		**InceptionLargeModel**	
Digits	**Joints**	**Accuracy**	**F1 Score**	**Accuracy**	**F1 Score**	**Accuracy**	**F1 Score**	**Accuracy**	**F1 Score**	**Accuracy**	**F1 Score**
Index Finger	**IndexMCP**	0.95	0.88	0.94	0.86	0.95	0.88	0.93	0.83	0.94	0.85
	IndexPIP	0.90	0.33	0.88	0.29	0.90	0.33	0.89	0.31	0.91	0.36
	Digit	0.96	0.92	0.96	0.92	0.94	0.86	0.93	0.85	0.96	0.92
Middle Finger	**MiddleMCP**	0.96	0.91	0.95	0.88	0.91	0.81	0.94	0.86	0.96	0.91
	MiddlePIP	0.85	0.25	0.83	0.22	0.89	0.31	0.84	0.24	0.89	0.31
	Digit	0.96	0.92	0.95	0.89	0.95	0.89	0.95	0.89	0.95	0.89
Ring Finger	**RingMCP**	0.83	0.53	0.80	0.50	0.78	0.53	0.81	0.59	0.86	0.59
	RingPIP	0.89	0.31	0.84	0.24	0.84	0.24	0.81	0.21	0.89	0.31
	Digit	0.88	0.72	0.91	0.79	0.83	0.70	0.85	0.71	0.89	0.76
Little Finger	**LittleMCP**	0.98	0.92	0.94	0.83	0.94	0.84	0.95	0.87	0.96	0.88
	Digit	0.99	0.97	0.99	0.96	0.94	0.84	0.96	0.90	0.99	0.96
Thumb	**ThumbMCP**	0.94	0.84	0.95	0.87	0.98	0.94	0.94	0.84	0.98	0.93
	ThumbPIP	0.89	0.31	0.89	0.31	0.89	0.31	0.89	0.31	0.94	0.44
	Digit	0.95	0.89	0.96	0.91	0.95	0.89	0.94	0.86	0.98	0.94
Overall		**0.95**	**0.88**	**0.96**	**0.90**	**0.92**	**0.84**	**0.93**	**0.85**	**0.95**	**0.90**

F Regression Statistical Analysis

We present in Table 4 the results of our statistical analysis looking at whether the performance of the InceptionLargerModel is greater than that of the InceptionExtrinsic model: Overall; For individual joints; and for each motion group. P-values in bold represent statistically significant results for the one-tailed non-parametric Wilcoxon Signed-Rank test with a threshold of $p = 0.05$, corrected via Bonferroni correction.

Table 4: Statistical Analysis for the performance of the InceptionLargerModel and InceptionExtrinsic model

Experiment	**Correlation Coefficient**		**MAE** (Degrees)		**NMAE**		**RMSE** (Degrees)		**NRMSE**	
	p-Value	**ES**	**p-Value**	**ES**	**p-Value**	**ES**	**p-Value**	**ES**	**p-Value**	**ES**
Overall (Per Task) ($n = 136$)	**< 0.00001**	**0.560**	**< 0.00001**	**−0.672**	**< 0.00001**	**−0.654**	**< 0.00001**	**−0.539**	**0.00004**	**−0.485**
Overall (Per Marker) ($n = 12$)	0.11	0.923	**0.022**	**−1.0**	**0.022**	**−1.0**	0.945	−0.744	1.0	−0.718
Individual Joints (IndexPIPFlxExt) ($n = 12$)	**0.00009**	**0.469**	**0.00044**	**−0.437**	**0.00044**	**−0.437**	**0.00023**	**−0.451**	**0.00023**	**−0.451**
Individual Joints (MiddlePIPFlxExt) ($n = 12$)	0.552	0.248	1.0	−0.215	1.04	−0.215	1.0	−0.186	1.0	−0.186
Individual Joints (RingPIPFlxExt) ($n = 12$)	1.0	0.0313	1.0	−0.193	1.0	−0.193	1.0	−0.165	1.0	−0.165
Individual Joints (LittlePIPFlxExt) ($n = 12$)	1.0	0.0981	1.0	−0.191	1.0	−0.191	1.0	−0.132	1.0	−0.132
Individual Joints (ThumbPIPFlxExt) ($n = 12$)	**< 0.00001**	**0.505**	**< 0.00001**	**−0.520**	**< 0.00001**	**−0.520**	**< 0.00001**	**−0.519**	**< 0.00001**	**−0.519**
Individual Joints (IndexMCPFlxExt) ($n = 12$)	**< 0.00001**	**0.598**	**< 0.00001**	**−0.573**	**< 0.00001**	**−0.573**	**< 0.00001**	**−0.548**	**< 0.00001**	**−0.548**
Individual Joints (MiddleMCPFlxExt) ($n = 12$)	**0.0048**	**0.383**	**0.00001**	**−0.509**	**0.00001**	**−0.509**	**0.00037**	**−0.441**	**0.00037**	**−0.441**
Individual Joints (RingMCPFlxExt) ($n = 12$)	0.854	0.232	0.331	−0.265	0.331	−0.265	0.224	−0.278	0.224	−0.278
Individual Joints (LittleMCPFlxExt) ($n = 12$)	**0.00022**	**0.452**	**0.00002**	**−0.502**	**0.00002**	**−0.502**	**0.00021**	**−0.453**	**0.00021**	**−0.453**
Individual Joints (ThumbMCPFlxExt) ($n = 12$)	**< 0.00001**	**0.575**	**< 0.00001**	**−0.551**	**< 0.00001**	**−0.551**	**< 0.00001**	**−0.550**	**< 0.00001**	**−0.550**
Individual Joints (ThumbAbdAdd) ($n = 12$)	**< 0.00001**	**0.555**	**< 0.00001**	**−0.680**	**< 0.00001**	**−0.680**	**< 0.00001**	**−0.674**	**< 0.00001**	**−0.674**
Individual Joints (WristFlxExt) ($n = 12$)	0.111	0.299	0.259	−0.273	0.259	−0.273	0.157	−0.289	0.157	−0.289
Motion Groups (Natural Motions) ($n = 12$)	1.0	0.371	1.0	−0.448	1.0	−0.371	1.0	−0.21	1.0	−0.0952
Motion Groups (Sign Language Motions) ($n = 12$)	1.0	0.5	1.0	−0.517	1.0	−0.533	1.0	−0.45	1.0	−0.433
Motion Groups (Two DoF Motions) ($n = 12$)	**0.00293**	**0.656**	**0.00005**	**−0.801**	**0.00005**	**−0.799**	**0.00376**	**−0.646**	**0.0471**	**−0.538**
Motion Groups (One DoF Motions) ($n = 12$)	**0.0109**	**0.585**	**0.00017**	**−0.737**	**0.00013**	**−0.745**	**0.00187**	**−0.653**	**0.00203**	**−0.650**

Statistical analysis of overall performance between the two models uses the metric (averaged over all the predicted joints) for each task per subject as the samples (n = 136). Statistical analysis of the performance

between the two models for predicted joints uses the metric (averaged over all tasks and subjects) for each predicted joint as the samples (n = 12). Statistical analysis of the performance between the two models for motion groups uses the metric (averaged over all tasks included in that motion group and subjects) for each predicted joint as the samples (n = 12).

Effect sizes (ES) are determined through the matched pairs rank-biserial correlation [3].

References

[1] Vicon. Vicon Gap Filling FAQ's;. http://www.vicon.com/support/faqs/?q=what-gap-filling-algorithms-are-used-nexus-2.

[2] Szegedy C, Ioffe S, Vanhoucke V, Alemi A. Inception-v4, inception-resnet and the impact of residual connections on learning. arXiv preprint arXiv:160207261. 2016.

[3] Kerby DS. The simple difference formula: An approach to teaching nonparametric correlation. Comprehensive Psychology. 2014;3:11-IT.